Tpr, a Large Coiled Coil Protein Whose Amino Terminus Is Involved in Activation of Oncogenic Kinases, is Localized To the Cytoplasmic Surface of the Nuclear Pore Complex

David A. Byrd,* Deborah J. Sweet,* Nelly Panté,§ Konstantin N. Konstantinov,‡ Tinglu Guan,* Andrew C.S. Saphire,* Philip J. Mitchell,‖ Colin S. Cooper,‖ Ueli Aebi,§¶ and Larry Gerace*

*Departments of Cell Biology and ‡Molecular and Experimental Medicine, The Scripps Research Institute, La Jolla, California 92037; §M.E. Muller Institute for Microscopy, Biozentrum, University of Basel, CH-4056 Basel, Switzerland; ‖Institute of Cancer Research, Sutton, Surrey, SM2 5NG, United Kingdom; and ¶The Johns Hopkins University School of Medicine, Baltimore, Maryland 21205

Abstract. From a panel of monoclonal antibodies raised against fractions of rat liver nuclear envelopes (NEs), we have identified an antibody, RL30, which reacts with novel nuclear pore complex (NPC) antigens that are not O-glycosylated. By immunofluorescence staining of cultured cells, RL30 reacts exclusively with the NE in a punctate pattern that largely coincides with that of identified NPC proteins. RL30 labels only the cytoplasmic surface of the NPC in immunogold electron microscopy, predominantly in peripheral regions nearby the cytoplasmic ring. In immunoblots of isolated rat liver NEs and cultured rat cells, RL30 recognizes a 265-kD band, as well as a series of 175–265-kD bands in rat liver NEs that are likely to be proteolytic products of p265. Sequencing of peptides from the 175- and 265-kD RL30 antigens of rat liver revealed that they are both closely related to human Tpr, a protein whose amino-terminal 150–250 amino acids appear in oncogenic fusions with the kinase domains of the *met*, *trk*, and *raf* protooncogenes. We found that in vitro translation of human Tpr mRNA yields a major 265-kD band. Considered together, these data indicate that the 265-kD RL30 antigen in the NPC is the rat homologue of Tpr. Interestingly, Tpr contains an exceptionally long predicted coiled coil domain (~1600 amino acids). The localization and predicted structure of Tpr suggest that it is a component of the cytoplasmic fibrils of the NPC implicated in nuclear protein import. Immunofluorescence microscopy shows that during NPC reassembly at the end of mitosis, Tpr becomes concentrated at the NE significantly later than O-linked glycoproteins, including p62. This indicates that reassembly of the NPC after mitosis is a stepwise process, and that the Tpr-containing peripheral structures are assembled later than p62.

NUCLEOCYTOPLASMIC transport is carried out by nuclear pore complexes (NPCs)[1] (reviewed by Forbes, 1992; Gerace, 1992; Panté and Aebi, 1993; Fabre and Hurt, 1994), large supramolecular structures that span the nuclear envelope (NE) at regions where the inner and outer nuclear membranes are joined. The NPC contains aqueous channels that provide conduits for nonselective passive diffusion of ions, metabolites, and other small molecules (Peters, 1986). Most proteins and RNAs are too large to diffuse through these channels at physiologically significant rates, and instead are actively transported through a gated channel in the NPC by selective, signal-mediated mechanisms (Forbes, 1992; Gerace, 1992; Panté and Aebi, 1993). Signal-mediated transport of macromolecules through the NPC is regulated, and can provide an important mechanism for control of gene expression (reviewed by Gerace, 1992; Whiteside and Goodbourn, 1993).

The NPC has dimensions of ~120 × 80 nm and a mass of ~125 × 10^6 D (Reichelt et al., 1990). Its framework consists of a central multidomain "spoke" assembly with peripheral "rings" on the cytoplasmic and nucleoplasmic surfaces (Hinshaw et al., 1992; Akey and Radermacher, 1993). This framework has eightfold rotational symmetry about an axis perpendicular to the nuclear surface and twofold symmetry about an axis parallel to the NE through the NPC center. A "central channel complex" (Gerace, 1992) of poorly defined architecture is attached to the inside of the spokes, and it contains a gated channel involved in signal-mediated import and export of macromolecules. Associated with this

Address all correspondence to Larry Gerace, The Scripps Research Institute, Department of Cell Biology, 10666 North Torrey Pines Road, La Jolla, CA 92037. Tel.: (619) 554-8514. Fax: (619) 554-6253.

1. *Abbreviations used in this paper*: NE, nuclear envelope; NPC, nuclear pore complex; NRK, normal rat kidney; ORF, open reading frame.

generally symmetrical framework are sets of eight fibrils emanating from both the nucleoplasmic and cytoplasmic rings (Jarnik and Aebi, 1991). In isolated amphibian oocyte NEs, the nucleoplasmic fibrils, which are ~75–100 nm long, are joined at their distal ends in a "terminal ring," while the structurally distinct cytoplasmic fibrils are <25–50 nm long and have no obvious distal connections (Jarnik and Aebi, 1991; Panté and Aebi, 1993).

Nuclear protein import is the best understood nuclear transport pathway. It is specified by short sequences in the transported proteins called nuclear localization sequences, which are usually enriched in basic amino acids (reviewed by Dingwall and Laskey, 1991). Studies involving the use of nuclear localization sequence–coated gold particles as probes to visualize transport in the EM (Feldherr et al., 1984) indicate that an early step in nuclear import involves ligand association with the cytoplasmic surface of the NPC, which can occur in the absence of ATP and at 0°C (Newmeyer and Forbes, 1988; Richardson et al., 1988). The initial sites of ligand association are suggested to involve the cytoplasmic fibrils of the NPC (Richardson et al., 1988; discussed by Gerace, 1992). Subsequent transport steps, which are ATP and temperature dependent (Newmeyer and Forbes, 1988; Richardson et al., 1988), involve channel gating and translocation of ligand to the nucleoplasmic side of the NPC. From biochemical analysis of nuclear import with in vitro assays, it has become clear that multiple cytosolic factors are involved (Adam et al., 1990; Newmeyer and Forbes, 1990; reviewed by Fabre and Hurt, 1994). To understand nuclear transport mechanisms, it will be of critical importance to characterize the structures and proteins of the NPC that interact with these cytosolic transport factors and the specific steps mediated by these components.

Currently only a relatively small number of the estimated 100–200 NPC polypeptides have been characterized in detail (reviewed by Fabre and Hurt, 1994). In vertebrates, these include at least eight polypeptides modified with O-linked *N*-acetylglucosamine (Snow et al., 1987; Davis and Blobel, 1987). The cDNA sequences have been determined for three of these O-linked glycoproteins: p62 (Starr et al., 1990), Nup153 (Sukegawa and Blobel, 1993), and CAN (Kraemer et al., 1994), a 214-kD polypeptide characterized previously as part of a fusion protein associated with a subtype of myeloid leukemia (von Lindern et al., 1992). At least some of the vertebrate O-linked glycoproteins appear to have a direct involvement in mediated transport through the NPC (reviewed by Gerace, 1992; Fabre and Hurt, 1994).

In this study, we report the characterization of a 265-kD protein of rat liver NEs that localizes to the NPC. We discovered that this protein is a rat homologue of human Tpr, a protein that has been previously detected in oncogenic fusions with the kinase domains of the *trk*, *met*, and *raf* protooncogenes (Park et al., 1986; Soman et al., 1991; Greco et al., 1992). Tpr contains an exceptionally long predicted coiled-coil α-helical region of ~1600 residues beginning near its NH_2 terminus, flanked by a highly acidic COOH-terminal region (Mitchell and Cooper, 1992*b*). Using immunogold EM, we found that Tpr is localized exclusively to the cytoplasmic surface of the NPC and is concentrated in regions near the cytoplasmic ring. The sequence properties and localization of Tpr suggest that it is a component of the cytoplasmic fibrils of the NPC, which may be involved in ligand docking. During NPC reassembly at the end of mitosis, Tpr becomes concentrated at the NE distinctly later than other O-linked glycoproteins including p62. This suggests that assembly of the NPC at the end of mitosis is a stepwise process in which peripheral structures containing Tpr assemble after the p62 glycoprotein.

Materials and Methods

Subcellular Fractionation of Rat Liver

Unless otherwise noted, all procedures were conducted at 0–4°C. Crude NEs were isolated from rat liver as described (Gerace et al., 1984). To isolate rat liver cytosol, rat liver homogenate was first centrifuged in a rotor (J6B; Beckman Instruments, Brea, CA) at 2,000 rpm for 10 min to yield a low speed supernatant. The latter was next centrifuged in a Beckman JA20 rotor at 10,000 rpm for 30 min to yield an intermediate speed supernatant. This supernatant was then centrifuged in a Beckman Ti45 rotor for 1 h at 40,000 rpm, yielding a supernatant comprising the rat liver cytosol fraction. The microsomal membrane fraction was prepared as described (Gerace et al., 1982). Protein concentrations for the various subcellular fractions analyzed in Fig. 1 were determined with a protein assay kit (Bio Rad Laboratories, Hercules, CA).

Crude NEs were fractionated by washing with 500 mM NaCl (Snow et al., 1987). Salt-washed NEs were extracted with 8 M urea as previously described (Foisner and Gerace, 1993). To solubilize NE proteins for immunoadsorption, salt washed NEs were resuspended at 100 OD U/ml (1 OD U of NEs is the amount derived from 1 OD_{260} of nuclei) in S buffer (50 mM Tris, pH 8.8, 500 mM NaCl, 2% Triton X-100, 10 mM EDTA, 1 mM DTT, 1 mM PMSF, and 1 μg/ml each of leupeptin, pepstatin, and aprotinin), incubated on ice for 30 min, and ultracentrifuged for 20 min at 65,000 rpm in a Beckman TLA100.2 rotor to yield a supernatant of solubilized proteins that was used directly for immunoadsorption (see below).

Cell Culture and Labeling

Normal rat kidney (NRK) and HeLa cells were grown at 37°C in Dulbecco's modified Eagle's medium (GIBCO BRL, Gaithersburg, MD) containing 10% fetal calf serum, 100 U/ml penicillin, and 100 μg/ml streptomycin. CHO cells were grown in Joklik's modified minimal essential medium (Gibco-BRL) containing nonessential amino acids, 10% fetal calf serum, and penicillin/streptomycin. For immunoadsorption, cells were grown to 75–90% confluency in 10-cm tissue culture dishes. Dishes were washed once in ice-cold PBS (40 mM NaCl and 10 mM sodium phosphate, pH 7.4) and cells were lysed in the dish by adding 1 ml of ice-cold S buffer (see above). The lysed cells were harvested with a rubber spatula, transferred to a microfuge tube, gently sonicated for 10 s, incubated on ice for another 30 min, and then centrifuged in a Beckman TLA100.2 rotor for 20 min at 65,000 rpm, yielding a supernatant of solubilized cell protein for immunoadsorption.

Metabolically labeled NRK cells were obtained by washing 10-cm plates grown to 75–90% confluency twice with methionine-deficient medium (ICN Biomedicals Inc., Irvine, CA), incubating the cells in the same medium for 30 min in a 37°C cell culture incubator, and then replacing the medium with 4 ml of methionine-deficient medium containing Tran^{35}S-label (ICN Biomedicals) at 0.5 mCi/ml. The cells were again incubated for 30 min in a 37°C incubator, the radioactive medium was removed, and the cells were solubilized as described above.

Antibody Production

The RL30 hybridoma line, which secretes antibodies against Tpr, was obtained by immunizing Armenian hamsters with an O-linked glycoprotein–enriched fraction of rat liver NEs and fusing the spleen cells of these animals with a mouse myeloma cell line as described (Foisner and Gerace, 1993). To obtain RL30 culture supernatant, the RL30 hybridoma was grown in EXCELL 300 serum-free medium (JRH Biosciences, Lenexa, KS) supplemented with penicillin and streptomycin. The supernatant was cleared of cells and cell debris by spinning the culture in a Beckman J6B rotor at 5,000 rpm for 20 min. Solid ammonium sulfate was slowly added to the supernatant to a final concentration of 55% and precipitated overnight at 4°C. The precipitated antibodies were pelleted, and pellets were resuspended in ice-cold PBS + 0.02% NaN_3 and were dialyzed against this buffer overnight with three changes. The RL30 antibodies in the concen-

trated culture supernatant were purified by binding to either HI Trap Protein G or GammaBind-Plus immunoaffinity columns (Pharmacia Biotech, Piscataway, NJ), which were washed with PBS and eluted with 200 mM glycine, pH 2.2 or 2.7, respectively. The eluant was immediately dialyzed against PBS + NaN_3 overnight with three changes, and was concentrated in a colloidian apparatus with 25,000 mol wt cutoff membrane (Schleicher & Schuell, Inc., Keene, NH).

Rabbit polyclonal antibodies specific for rat p62 have been characterized previously (see Fig. 4 in Snow et al., 1987). For the experiments in this paper, the antibodies were affinity-purified on a column of recombinant rat p62 obtained by expression in *Escherichia coli*, instead of using the p62 band excised from an immunoblot as described previously (Snow et al., 1987). Recombinant p62 was provided by Bryce Paschal (The Scripps Research Institute, La Jolla, CA), who expressed it using a p62 cDNA obtained from John Hanover (Laboratory of Biochemistry and Metabolism, National Institute of Diabetes and Digestive and Kidney Diseases, Bethesda, MD) (Starr et al., 1990).

Immunoadsorption, SDS Gel Electrophoresis, and Immunoblotting

To prepare a solid-phase RL30 immunoadsorbent, purified RL30 antibodies were dialyzed and concentrated against coupling buffer consisting of 200 mM sodium carbonate, pH 8.9, and 500 mM NaCl, and then coupled to cyanogen bromide–activated Sepharose 4B (Pharmacia Biotech) at a ratio of 4 mg of antibody/ml of beads according to the manufacturer's instructions. After blocking with 100 mM ethanolamine, the beads were washed three times in PBS + 0.02% NaN_3 and stored at 4°C. 15 μl of RL30-Sepharose were prewashed in 500 μl S buffer and then incubated overnight with either 1 ml of whole cell lysate or 100 ODs of solubilized salt washed NEs (see above). The beads were then washed three times in S buffer, once in S buffer without Triton X-100, and eluted in SDS gel sample buffer containing 100 mM DTT for 10 min at 37°C.

Samples of subcellular fractions and immunoadsorbed proteins were separated on either precast 4–15% gradient SDS polyacrylamide gels (Bio Rad Laboratories) or on 5% SDS polyacrylamide gels, using the sample preparation conditions described previously (Gerace et al., 1982). For immunoblotting, proteins in gels were electrophoretically transferred onto supported nitrocellulose (Micron Separations Inc., Westborough, MA). These blots were blocked in TBST (50 mM Tris-HCl, pH 7.9, 150 mM NaCl, and 0.05% Tween 20) containing 2% BSA (TBST-BSA) for 1 h at room temperature, and were then incubated with primary antibody solutions for 1 h at room temperature or overnight at 4°C. Primary antibodies were all diluted in TBST-BSA buffer and consisted of either purified RL30 at a concentration of 5 μg/ml, RL1 ascites, or human autoimmune patient serum No. 30 diluted 1:500, or rabbit polyclonal antipeptide sera raised against the human Tpr peptide LNKLPKSVQNKLE (comprising residues 14-26) diluted 1:200. After primary antibody incubations, the blots were washed three times for 5 min in TBST-BSA, and then incubated for 1 h at room temperature with alkaline phosphatase–coupled goat anti-human, goat anti-mouse IgG, and goat anti-rabbit antibodies (Promega Corp., Madison, WI) all diluted 1:4,000 in TBST-BSA. Since the goat anti-mouse antibodies obtained from Promega cross-reacted with the RL30 Armenian hamster antibodies, no mouse anti-hamster bridge antibody was required. After secondary antibody incubations, the blots were washed three times for 5 min in TBST and once in TBST lacking Tween 20, and were then developed with nitroblue tetrazolium/bromochloroinodyl phosphate alkaline phosphatase buffer as described (Harlow and Lane, 1988). The colorimetric reactions were stopped by extensive washing of the blots with water.

Peptide Sequencing

To obtain peptide sequences, RL30 antigens were immunoadsorbed from 4000 ODs of rat liver NEs and were electrophoresed on a 5% SDS-polyacrylamide gel. The proteins contained in the gel were then electrophoretically transferred onto an Immobilon polyvinyldifluoride membrane (Millipore Corp., Bedford, MA) overnight at 4°C in buffer containing 100 mM Tris, pH 8.8, and 100 mM boric acid. The blot was stained with 0.1% Ponceau S in 1% acetic acid, and indicator strips were removed and analyzed by immunoblotting with RL30 as described above. Horizontal strips of the membrane corresponding to the p175 and p265 bands were excised and digested with endoproteinase Lys C (Sigma Immunochemicals, St. Louis, MO). The peptides then were eluted from the membrane and separated on a C_{18} reversed-phase HPLC column. Seven peak fractions were subjected to automated Edman degradation on a sequencer (model 4777A; Applied Biosystems, Inc., Foster City, CA) equipped with an in-line PTH analyzer (model 120A; Applied Biosystems). Peptide sequences obtained were used to search the GenEMBL database using the TFASTA search program (Genetics Computer Group, Madison, WI). Protease digestion, HPLC purification, and peptide sequencing were carried out by Dr. John Leszyk (Protein Chemistry Facility, Worcester Foundation for Experimental Biology, Worcester, MA).

Construction and Expression of Full-length Tpr

A full-length Tpr cDNA was assembled from three partial length cDNA clones: λHT5, λHT9, and λHT14 (Mitchell and Cooper, 1992*b*). First, the BstXI site in the multiple cloning site of pBluescript-SK was destroyed by digesting with BstXI, carrying out 5′-3′ exonuclease digestion with Klenow fragment, and religating the plasmid. The 2.5-kb EagI-EcoRI fragment from the 5′ partial-length cDNA λHT5 was subcloned into the BstXI-lacking pBluescript-SK and renamed pH T5. Two complementary oligonucleotides which code for an amino terminal *c-myc* epitope with the sequences 5′-CGACATGGCAGAGGAGCAAAAACTTATTTCTGAAGAGGACTTGCTTAAGGG-3′ and 3′-TACCGTCTCCTCGTTTTTGAATAAAGACTTCTCCTGAACGAATTCCCGCTG-5′ were annealed and inserted into the cDNA BstXI site at nucleotide 294, resulting in the plasmid pMyc5, which was sequenced to confirm the orientation and fidelity of the oligonucleotide insert. λHT14, which contains a 4.5-kb 3′ partial-length cDNA for Tpr, was double digested with NotI, which has a single site in the vector, and Psp1406I, which cuts the cDNA at nucleotide 4296. pMyc5 was cut with NotI in the multiple cloning site and with Psp1406I at nucleotide 2466, releasing a 2.2-kb cDNA fragment that was ligated into the NotI-Psp1406I linearized λHT14, resulting in pMyc5-14. The 1.8-kb Psp1406I cDNA fragment from λHT9 was ligated into pMyc5-14, which was linearized with Psp1406I, resulting in the full-length construct pMycTpr. T7 promoter, SalI, and KpnI sequences were introduced into pMycTpr by annealing and ligating the complementary oligos T71, 5′-GGCCTAATACGACTCACTATAGGGTCGACGG TACCGC-3′, and T72, 3′-ATTATGCTGAGTGATATCCCAGCTGCCATGGCGCCGG-5′, into the NotI site of pMycTpr. Sequencing confirmed the orientation and fidelity of the oligonucleotides. The correct construct was called pT7Tpr and was used for in vitro translation.

For DNA sequencing and in vitro transcription/translation of the full-length Tpr construct, pT7Tpr plasmid DNA was purified using the Maxi-Prep Kit (QIAGEN Inc., Chatsworth, CA). DNA sequencing was carried out using a PRISM™ cycle sequencing kit and the model 373A DNA sequencing system (Applied Biosystems). The sequence around the originally predicted stop codon was determined by first subcloning two fragments of Tpr cDNA [XbaI(6415)-HindIII(7496) and NsiI(4458)-SphI(6620)] into pBluescript-SK+ (Stratagene, La Jolla, CA) and sequencing using M13 reverse and forward primers, respectively. For in vitro translation, the full-length construct with the T7 RNA polymerase promoter was used in the TnT T7 coupled reticulocyte lysate system (Promega). 1.5 μg of purified pT7Tpr plasmid DNA was used in a 50-μl reaction with tran^{35}S-label. 40 μl of the reaction was loaded on the 5% SDS-PAGE gel shown in Fig. 3 *b*.

Immunofluorescence Microscopy

NRK or HeLa cells were grown as described above on No. 1 coverslips. The coverslips were washed twice in PBS, fixed for 5 min in PBS containing 1.1 or 4% paraformaldehyde for visualizing interphase or mitotic cells, respectively, washed three times with PBS, and then permeabilized for 6 min in PBS + 0.2% Triton X-100. After permeabilization, they were washed three times with PBS and twice with PBS + 0.2% gelatin (PBS-G). For detection of the RL30 Armenian hamster antibodies in immunofluorescence microscopy, purified mouse monoclonal anti-hamster IgG, RG7/7, was used as a bridge antibody. For double immunofluorescence experiments, primary antibody solutions (all in PBS-G) consisted of purified RL30 antibodies at 20 μg/ml, purified RG7/7 at 2 μg/ml, and either mouse IgM RL1 ascites diluted 1:500, rabbit anti-lamin serum diluted 1:400, or affinity-purified rabbit anti-p62 antibodies. The coverslips were incubated with the primary antibody solutions for 30 min at room temperature in a humidified chamber. The coverslips were then washed three times with PBS and twice with PBS-G. The secondary antibody solutions (all in PBS-G) contained rhodamine-coupled, affinity-purified goat anti-mouse IgG diluted 1:200 and either fluorescein-coupled, affinity-purified donkey anti-rabbit antibodies at 1:100 or fluorescein-coupled, affinity-purified goat anti-mouse IgM diluted 1:100. All secondary antibodies were from Jackson Immunoresearch, Inc. (West Grove, PA). The coverslips were incubated with the secondary antibodies for 30 min, and were washed twice with PBS,

once in PBS-G, and inverted over a solution containing 50% PBS, 50% glycerol, and SlowFade antifade agent (Molecular Probes, Inc., Eugene, OR). Samples were examined with an Axiophot microscope (Carl Zeiss, Inc., Thornwood, NY) or a laser scanning confocal microscope (MRC-600; Bio-Rad).

Immunogold Electron Microscopy

Colloidal gold particles, ~8 nm in diameter, were prepared by reduction of tetrachloroauric acid with sodium citrate in the presence of tannic acid (Slot and Geuze, 1985). The monoclonal antobody RL30 was conjugated to colloidal gold particles as described by Baschong and Wrigley (1990). After conjugation, the complexes were dialyzed agains PBS and centrifuged at 45,000 *g* for 15 min. The soft pellet was resuspended in STM buffer (10% sucrose, 10 mM Hepes, pH 7.4, 1 mM $MgCl_2$, and 1 mM DTT) and used for labeling rat liver NEs.

For immunogold labeling, pellets of crude rat liver NEs were resuspended in STM buffer at about 50 OD/ml, and the gold-conjugated RL30 was added to this suspension at a final concentration of ~5 μg/ml. After incubation for 1 h at room temperature, the labeled NEs were salt washed by adding an equal volume of STM buffer containing 1 M NaCl, followed by centrifugation for 5 min in an Eppendorf microfuge at 5,000 *g*. The pellets of NEs were then washed very gently (without further centrifugation) three times for 10 min each with STM buffer containing 1% BSA.

After immunogold labeling and washing, samples were fixed with 2% glutaraldehyde in PBS at 4°C for 30 min, washed three times with cold PBS, and postfixed for 1 h with 1% OsO_4 in PBS at 4°C. Next the samples were dehydrated and embedded in Epon 812 resin as described by Jarnik and Aebi (1991). Thin sections were cut on a microtome (Ultracut; Reichert-Jung Optische Werke, Vienna, Austria) using a diamond knife. The sections were collected on carbon/colloidon-coated EM grids, stained with 6% uranyl acetate for 45 min, and poststained with 2% lead citrate for 1 min (Millonig, 1961). Specimens were examined under a transmission electron microscope (H-8000; Hitachi Scientific Instruments, Mountain View, CA) operated at an acceleration voltage of 75 kV. Micrographs were recorded on SO-163 film (Eastman Kodak Co., Rochester, NY). Magnification calibration was performed according to Wrigley (1968) using negatively stained catalase crystals.

Results

A Monoclonal Antibody That Recognizes a Group of Novel Nuclear Envelope Antigens

From a panel of monoclonal antibodies against fractions of rat liver NEs (see Materials and Methods), we identified one antibody, RL30, that appeared to react specifically with the NPC in immunofluorescence microscopy (see below). On immunoblots of isolated rat liver NEs, RL30 recognized a group of bands migrating between 175 and 265 kD, including major bands at ~175 kD (p175), 225 kD, and 265 kD (p265) (Fig. 1, lanes *5*). These bands were observed in a large number of different rat liver NE preparations and experiments,

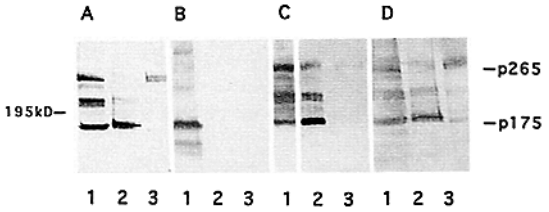

Figure 2. Immunoblot analysis of RL30 antigens. Fractions analyzed are salt-washed rat liver NEs (lanes *1*), RL30 antigens immunoadsorbed from solubilized rat liver NEs (lanes *2*), and RL30 antigen immunoadsorbed from solubilized NRK cells (lanes *3*). Immunoblots of these fractions were probed with RL30 (*A*), RL1 (*B*), human autoimmune serum No. 30 (*C*), and a polyclonal antibody against residues 14-26 of human Tpr (*D*). All of the immunoreactivity shown in *D* was abolished by including a peptide containing residues 14-26 of Tpr in the primary antibody incubation (data not shown).

although additional immunoreactive bands in the 175–265-kD region were obtained frequently. The relative proportion of the three major antigens detected by immunoblotting varied with different preparations. In some cases (Fig. 1), p175 was apparently more abundant than p265, while in other cases (Fig. 2), they were equally abundant. As discussed further below, it is likely that most or all of the RL30 antigens migrating faster than the 265-kD band from rat liver NEs are produced by in vivo and/or in vitro proteolysis of p265.

The major RL30 antigens were highly enriched in isolated NEs in comparison to other subcellular fractions. While they were readily detected in isolated NEs by immunoblotting (Fig. 1, lanes *5*), they were undetectable in cytosol, microsomal membranes, isolated nuclei, or DNAase-released nuclear contents (Fig. 1, lanes *1–4*). RL30 reacted weakly with an ~40-kD band enriched in the cytosol fraction (Fig. 1), but its relationship to the 175–265-kD NE antigens is unknown. The RL30 antigens of NEs were tightly envelope-associated, as they were not substantially released into a supernatant by extraction with 0.5 M NaCl, which solubilizes most contaminating chromatin (Fig. 1, lanes *6* and *7*) (Snow et al., 1987). However, when NEs were extracted with 8 M urea, the RL30 antigens were completely solubilized (Fig. 1, lanes *8* and *9*), indicating that they are peripheral membrane proteins of the NE.

The multiple 175–265-kD RL30-reactive bands detected in unfractionated rat liver NEs by immunoblotting were all immunoadsorbed by RL30 from NEs solubilized in Tri-

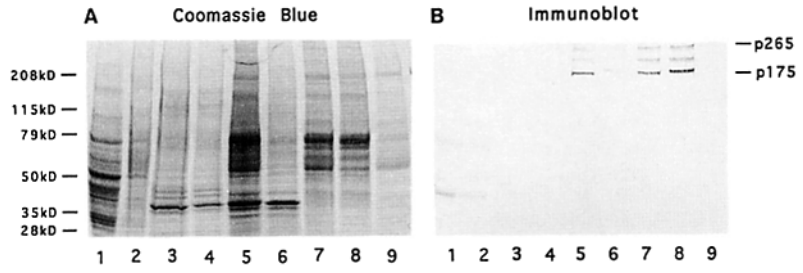

Figure 1. Distribution of Tpr in subcellular fractions of rat liver. Samples of subcellular fractions of rat liver were separated on a 4–15% gradient SDS polyacrylamide gel and analyzed by staining with Coomassie blue (*A*) or immunoblotting with the RL30 monoclonal antibody (*B*). Lanes *1–4* contain 50 μg of the following samples: cytosol (lanes *1*), microsomal membranes (lanes *2*), isolated nuclei (lanes *3*), and nuclear contents released from nuclei by nuclease digestion at low ionic strength (lanes *4*). Lanes *5–9* contain ~4.5 × 10^7 nuclear equivalents of crude NEs (lanes *5*), the supernatant derived from extraction of crude NEs with 0.5 M NaCl (lanes *6*), the pellet of 0.5 M NaCl-washed NEs (lanes *7*), the supernatant from extraction of salt-washed NEs with 8 M urea (lanes *8*), and the pellet from extraction of NEs with 8 M urea (lanes *9*). Migrations of molecular mass standards are indicated on the left, and migrations of the p175 and p265 RL30 antigens are indicated on the right.

ton/high salt buffers (Fig 2 *A*, lanes *1* and *2*), although the relative amount of p175 increased relative to the upper bands during the immunoadsorption, presumably as a result of in vitro degradation. By contrast, when RL30 antigens were immunoadsorbed from a cultured rat cell line (NRK cells), a predominant doublet near 265 kD (Fig 2 *A*, lane *3*) or a single 265-kD band (Fig. 3) were detected, together with minor faster migrating bands. RL30 did not recognize cross-reacting antigens in CHO (hamster) and HeLa (human) cultured cells by immunoblotting or immunofluorescence microscopy (data not shown).

A number of experiments indicated that the RL30 antigens did not correspond to previously characterized NPC polypeptides. The immunoadsorbed RL30 antigens from rat liver and normal rat kidney (NRK) cells were not recognized by the RL1 monoclonal antibody (Fig. 2 *B*, lanes *2* and *3*), which reacts with a group of eight O-glycosylated NPC proteins (Snow et al., 1987). These include prominent bands migrating near 180 and 210 kD (Snow et al., 1987), which apparently correspond to Nup153 (Sukegawa and Blobel, 1993) and CAN (Kraemer et al., 1994), respectively, based on the gel mobility. Moreover, the rat liver RL30 antigens were not bound to wheat germ agglutinin–Sepharose (data not shown), which also recognizes the O-linked NPC glycoproteins, or to lentil lectin–Sepharose (data not shown), which binds to N-glycosylated proteins, including gp210 (Gerace et al., 1982). Interestingly, we found that the RL30 antigens were relatively prominent human autoimmune antigens. In a collection of 55 human autoimmune sera that react with the NE by immunofluorescence microscopy (Konstantinov et al., 1995), nine sera were found to react specifically with the group of antigens immunoadsorbed by RL30 (e.g., Fig. 2 *C*).

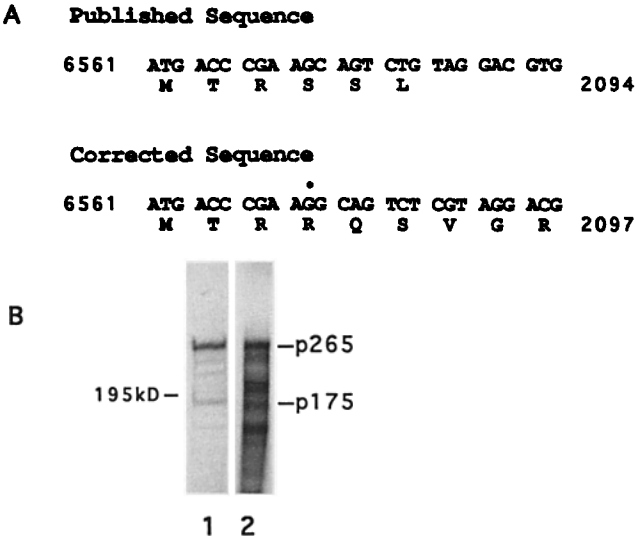

Figure 3. Corrected cDNA sequence of human Tpr near the originally predicted stop codon. (*A*) The top line shows the originally published cDNA and amino acid sequences near the predicted stop codon. The bottom line shows the corrected cDNA sequence, containing the insertion of a guanine nucleotide at nucleotide 6571. This results in an open reading frame that extends another 258 residues. (*B*) Lane *1* shows a sample immunoadsorbed from metabolically labeled NRK cells with RL30, in which p265 predominates. Lane *2* shows radiolabeled products from in vitro translation of a full-length cDNA from human Tpr, where a major 265-kD band is apparent.

Homology of the Rat Liver RL30 Antigens to Human Tpr

To further characterize the RL30 antigens, we immunoadsorbed the proteins from rat liver NEs and obtained sequences of peptides from the p175 and p265 bands (Table I; see Materials and Methods). Seven peptide sequences were obtained, five from p175 and two from p265 (Table I). All seven peptides were highly homologous to regions between residues 125 and 1518 of the predicted amino acid sequence of the human translocated promoter region (Tpr) protein (Mitchell and Cooper, 1992*b*). The HPLC profiles of proteolytic digests of p175 and p265 used for peptide sequencing were very similar (data not shown), further suggesting that the two bands are closely related structurally. In addition, polyclonal antibodies raised against a peptide comprising residues 14-26 of human Tpr reacted with the same bands as RL30 in rat liver NEs and a sample of immunoisolated RL30 antigens (Fig. 2 *D*). Considered together, these results indicate that p175 and p265 are different forms of a rat homologue of human Tpr.

The published sequence of human Tpr cDNA predicts an open reading frame (ORF1) encoding 2094 amino acids,

Table I. Comparison of Amino Acid Sequences of Peptides from Rat RL30 Antigens with Predicted Amino Acid Sequences from Human Tpr cDNA

Source of peptide	Amino acid sequence	Human Tpr amino acid No.
Rat p175	XḊLIXTNEXLXṠEVĖYL	
	||| ||| | |:|||	
	RDLIRTNERLSQELEYL	125-141
	LQḞQVEILTK	
	|| || |	
	LQKHVEDLLTK	250-260
	LLXEK	
	|| ||	
	LLLEK	409-414
	LGGQNILLK	
	|||:|||	
	QRGQNLLLK	809-817
	VIQQLNEEVGRLK	
	||||:||:||||	
	RIQQLTEEIGRLK	1367-1379
Rat p265	LSEVRLSQQRESLLA	
	|||||||||||||||	
	LSEVRLSQQRESLLA	793-807
	TLSEKETEARXLQEQṪÄQL	
	||||||||| |||||:||	
	TLSEKETEARNLQEQTVQL	1503-1518

X, unassignable; •, uncertain assignment; |, identical; :, conservative substitution.

with a predicted molecular mass of 238,513 D (Mitchell and Cooper, 1992*b*). However, a second distinct 299 residue ORF (ORF2) occurs at the 3′ end of the cDNA, which extends 254 amino acids beyond the predicted stop codon (Mitchell and Cooper, 1992*b*). In vitro translation of 3′ truncations of a Tpr cDNA segment (beginning at codon 1745 and extending up to 589 nucleotides downstream of the predicted stop at codon 2094) indicated that the actual translation stop site of Tpr was ≥20 kD downstream of the predicted stop (data not shown). Therefore, we resequenced the region surrounding the putative stop codon in a partial length cDNA clone containing this 3′ region (Mitchell and Cooper, 1992*b*). From this, we identified a sequencing error in codon 2092 of Tpr (Fig. 3 *A*), which introduces a one-nucleotide frameshift and results in a predicted stop three codons later. The corrected sequence in codon 2092 (Fig. 3 *A*) places ORF2 in frame with the main portion of Tpr, adding 258 residues of ORF2 onto the first 2091 amino acids of the previously described Tpr. With this correction, Tpr is now predicted to encode a 2349-residue protein with a predicted molecular mass of 265,559 D, which is close to the observed mobility of p265.

To directly investigate whether rat p265 comigrates with full-length Tpr, we assembled a full-length cDNA from three partial length clones, and we inserted a T7 RNA polymerase promoter and c-*myc* tag at the 5′ end of the full-length construct (see Materials and Methods). This construct was transcribed and translated in vitro with T7 RNA polymerase and reticulocyte lysate, and the size of the translation product was compared with the mobility of p265 immunoadsorbed from metabolically labeled NRK (normal rat kidney) cells. As shown in Fig. 3 *B*, p265 from the radiolabeled NRK cells comigrated with the largest and most abundant translation product. Moreover, when the Tpr cDNA with the c-*myc* tag was expressed in vivo in BHK cells using the vaccinia T7 RNA polymerase system, the largest product recognized by an anti-*myc* monoclonal antibody was a 265-kD band (data not shown). From these data, we conclude that the Tpr cDNA encodes a 265-kD protein, which corresponds to the 265-kD band of rat liver NEs and NRK cells recognized by RL30. Since all RL30-reactive bands migrating faster than p265 in rat liver NEs contain a Tpr epitope corresponding to residues 14-26 of human Tpr, these bands probably arise from proteolytic removal of different portions of the acidic COOH-terminal tail of the 265-kD full-length Tpr. This interpretation is consistent with the presence in this domain of several regions containing repeating PEST sequence motifs (Mitchell and Cooper, 1992*b*), which give rise to elevated protease sensitivity (Rogers et al., 1986).

Tpr Localization to the Cytoplasmic Surface of the Nuclear Pore Complex

In immunofluorescence microscopy of NRK cells, RL30 labeled the NE exclusively (Fig. 4). This was most clearly seen in confocal images near the nuclear equator, where all immunoreactivity occured at the nuclear "rim" (Fig. 4 *E*), similar to the labeling obtained with RL1 (Fig. 4 *F*), an antibody that reacts with O-linked glycoproteins of the NPC (Snow et al., 1987). In optical sections containing the nuclear surface, RL30 gave discontinuous punctate labeling of the NE (Fig. 4 *A*) that largely colocalized with RL1 staining (Fig. 4 *B*).

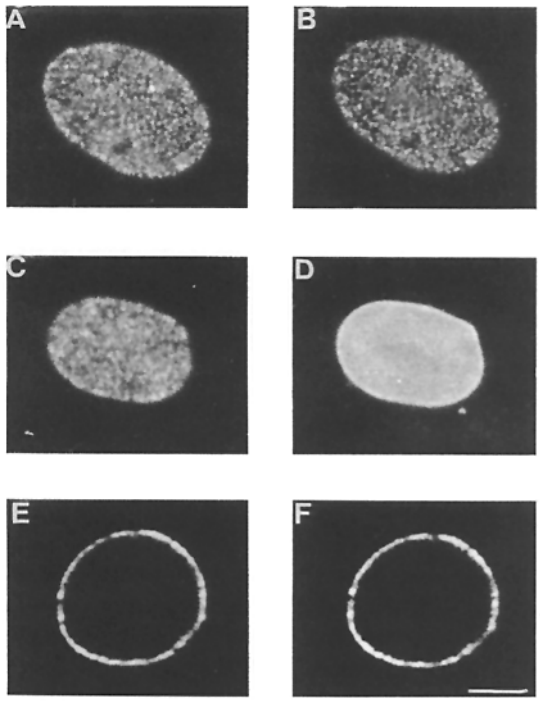

Figure 4. Localization of RL30 antigens in cultured rat NRK cells by immunofluorescence microscopy. NRK cells were fixed with formaldehyde, permeabilized with Triton X-100, and processed for double immunofluorescence labeling with RL30 and RL1 (*A* and *B*, respectively, and *E* and *F*, respectively) and RL30 and polyclonal anti-lamins A and C (*C* and *D*, respectively). Micrographs of nuclear surfaces (*A–D*) were taken with a conventional epifluorescence microscope, while images of equatorial regions of nuclei (*E* and *F*) were obtained with a confocal laser scanning microscope. Bar, 5 μm.

By contrast, the discontinuous RL30 labeling (Fig. 4 *C*) was distinct from the largely continuous labeling of the nuclear surface obtained with a polyclonal antibody to nuclear lamins (Fig. 4 *D*). Immunofluorescence labeling of human HEp-2 cells with several autoantibodies directed against the RL30 antigens (including the antibody characterized in Fig. 2 *C*) gave an essentially identical immunofluorescence localization pattern (data not shown). Hence, immunofluorescence microscopy indicates that Tpr is specifically localized to the NPC.

To examine the localization of RL30 antigens at higher resolution, we performed immunogold electron microscopy on isolated rat liver NEs with gold-conjugated RL30. As shown in Fig. 5, RL30 strongly and specifically labeled the NPC, and did not significantly decorate the lamina or other membrane components. Furthermore, RL30-gold labeling was found exclusively on the cytoplasmic surface of the NPC and was absent from the nucleoplasmic surface. The labeling was concentrated nearby and peripheral to the cytoplasmic ring, although labeling was occasionally seen in more central NPC regions (Fig. 5). This pattern of labeling is consistent with Tpr being part of the fibrils that emanate from the cytoplasmic ring of the NPC, which are occasionally bent and extend towards the center of the pore (Jarnik and Aebi, 1991). Taken together, the results of immunofluorescence

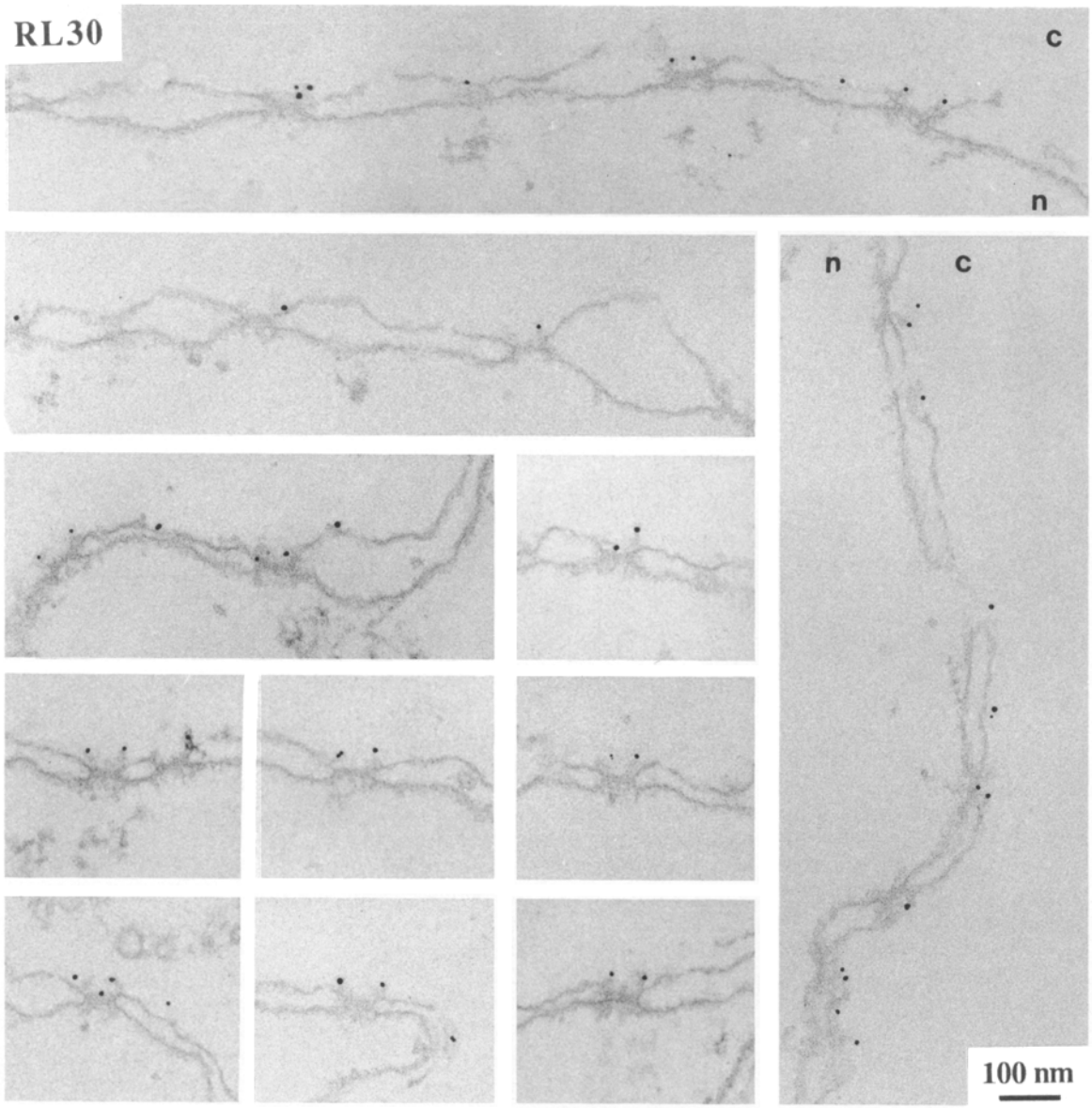

Figure 5. Localization of RL30 antigens in isolated rat liver nuclear envelopes by immunogold electron microscopy. Isolated nuclear envelopes were fixed, incubated with RL30-gold conjugates, embedded, and examined by thin section electron microscopy (see Materials and Methods). Shown are several views along single NEs, as well as a gallery of selected NPCs, to depict typical patterns of gold labeling obtained in areas containing well-preserved NPCs. The nucleoplasmic (*n*) and cytoplasmic (*c*) surfaces of the NE are indicated in the top and right images. The two nuclear membranes can be readily distinguished in these preparations because the outer nuclear membrane, unlike the inner membrane, is frequently ruptured.

and immunoelectron microscopy plus subcellular fractionation demonstrate that Tpr is a component of the NPC restricted to its cytoplasmic surface.

Late Assembly of Tpr in the Nuclear Envelope at the End of Mitosis

During mitosis, the NPC is disassembled at the ultrastructural level and component proteins are dispersed throughout the cytoplasm, as can be visualized by immunofluorescence microscopy of cultured cells (Forbes, 1992; Gerace, 1992). The NPC reassembles in the NE at the end of mitosis, when NPCs are inserted into the continuous double membrane surrounding chromatin masses. As illustrated in Fig. 6, in double immunofluorescence staining of mitotic NRK cells with RL1 and RL30, both groups of antigens became dispersed more or less diffusely throughout the cytoplasm in late prophase at the time of NE disassembly, and remained in a dispersed state throughout metaphase and anaphase. However, in late anaphase and early telophase when nuclear membranes are reassembled around mitotic chromsomes (Foisner and Gerace, 1993), RL1 antigens became progressively concentrated around the periphery of the chromosomes, while RL30 antigens remained dispersed throughout the cytoplasm (Fig. 6). Almost all of the RL1 antigens were concentrated at the chromosome surfaces before detectable

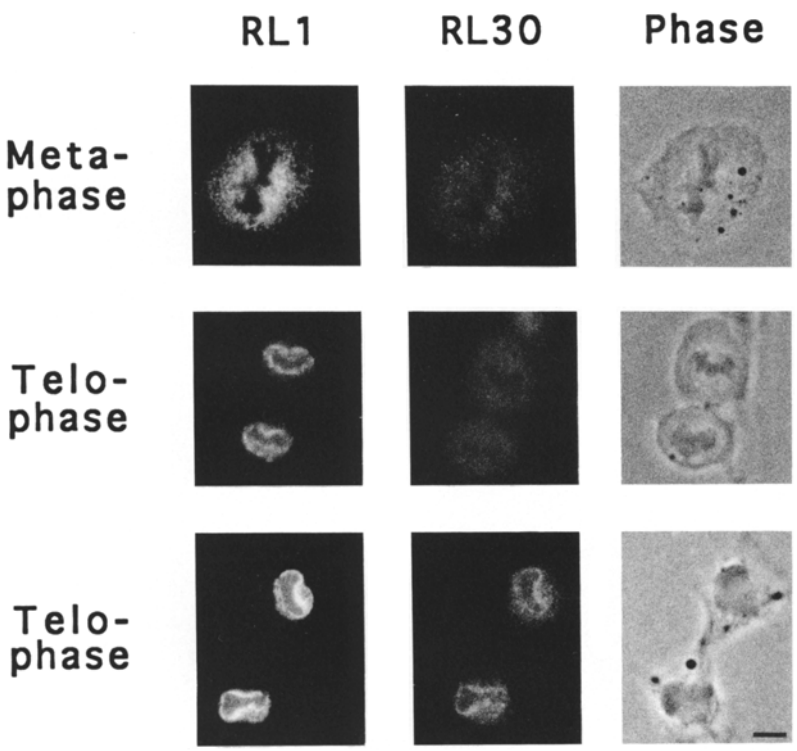

Figure 6. Double immunofluorescence localization of RL30 and RL1 antigens at the end of mitosis. NRK cells were processed for double immunofluorescence staining as in Fig. 4. Fluorescent and phase contrast images of cells in metaphase and progressive stages of early-late telophase are shown. Bar, 5 μm.

accumulation of RL30 antigens, which occurred only during mid-late telophase (Fig. 6). Similar results were obtained in double immunofluorescence staining of cells with RL30 and a polyclonal antibody that is monospecific for p62, one of the eight glycoproteins recognized by RL1 (Fig. 7). As before, most RL30 antigens became concentrated at the reforming NE after p62. These data suggest that assembly of the NPC is a stepwise process in which Tpr-containing peripheral structures assemble after other components, including p62.

Discussion

A Rat Homologue of Human Tpr

Using the RL30 monoclonal antibody, we have identified a 265-kD polypeptide of the NE that is a rat homologue of the previously described human Tpr protein, and have demonstrated that it is localized to the cytoplasmic surface of the NPC. Several criteria established that p265 corresponds to Tpr. First, the sequences of seven peptides from p265 and its putative proteolytic product p175 were highly homologous to sequences of human Tpr, with the extent of incomplete homology being compatible with the rat–human species difference. Second, in vitro translation of human Tpr cDNA yielded a product that comigrated with rat p265. Third, anti-peptide antibodies against human Tpr recognized the same rat liver NE antigens as RL30. The RL30-reactive bands migrating between 175 and 265 kD in rat liver NEs are likely to be in vivo and/or in vitro proteolytic products of p265, as suggested by their variable abundance in different preparations and by the predominance of the 265-kD band in NRK cells. Further supporting this interpretation, extensive analysis of human Tpr cDNAs from several libraries does not reveal distinct Tpr-related open reading frames that could account for the multiple 175–265-kD species (Mitchell and Cooper, 1992*a*, *b*).

In the course of our studies, we identified an error in the previously published sequence of human Tpr (Mitchell and Cooper, 1992*b*) at codon 2092, which causes a one-nucleotide frameshift and results in a predicted stop three codons later. A second distinct open reading frame was previously described in the Tpr cDNA that extends ~250 residues beyond the originally predicted stop site (Mitchell and Cooper, 1992*b*). With our sequence correction, the latter region is now placed in frame with the main body of the Tpr sequence. Thus, the corrected cDNA sequence predicts that Tpr is a 2349-residue protein with a molecular mass of 265,559 D.

The primary sequence of Tpr indicates the existence of at least two separate domains in this polypeptide (Fig. 8; see Mitchell and Cooper, 1992*b*). Most of the region between residues 50 and 1630 contains heptad repeats that are predicted to form a coiled-coil α-helix, although there are several segments ≤50 residues long interspersed throughout this region that have low coiled-coil potential (Fig. 8 *B*). This coiled coil domain is followed by a 700-residue hydrophilic domain enriched in acidic residues (16.7% aspartic + glutamic acid), serine (12.4%), and threonine (10.4%), with a predicted isoelectric point of 4.04. Tpr does not contain short repeat motifs, which seem to be characteristic of the mammalian O-linked glycoproteins (Starr et al., 1990; Sukegawa and Blobel, 1993; Kraemer et al., 1994). The only other characterized NPC protein predicted to form a coiled coil α-helix is p62, which contains an ~150 residue α-helical region with heptad repeats at its COOH terminus (Starr et al., 1990). The long predicted coiled coil region of Tpr could be involved in dimerization, with the protein form-

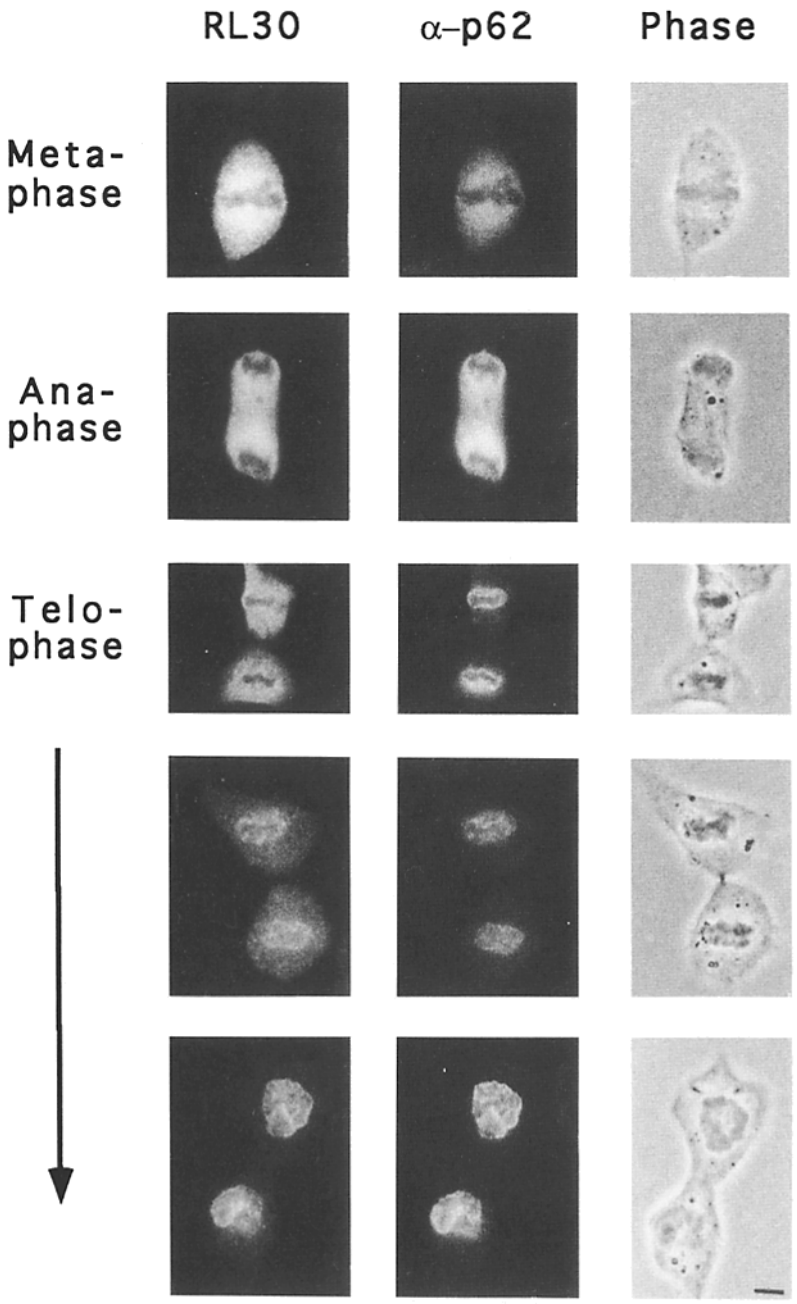

Figure 7. Double immunofluorescence localization of RL30 antigens and p62 at the end of mitosis. NRK cells were processed for double immunofluorescence staining as in Fig. 4. Fluorescent and phase contrast images of cells in metaphase, anaphase, and three progressive stages of telophase are shown. Bar, 5 μm.

ing a myosin-like homotypic dimer of parallel unstaggered monomers.

The ~140–230 NH_2-terminal residues of Tpr are found in oncogenic fusions with the kinase domains of three different protooncogenes: the receptor tyrosine kinases Met (Park et al., 1986; Soman et al., 1991) and Trk (Greco et al., 1992), as well as the cytoplasmic serine/threonine kinase Raf (Ishikawa et al., 1987). How fusion of the amino terminus of Tpr to tyrosine and serine kinase domains generates oncogenic fusion proteins is not entirely clear. One possibility is that the amino terminal region of Tpr mediates dimerization of the kinase domains and thereby mediates kinase activation (Rodriguez and Park, 1993; Sawyers and Denny, 1994). In a second and not mutually exclusive mechanism, the amino terminus of Tpr could serve to target the Trk, Raf, and Met kinases to the NPC, and this localized concentration of kinase activity could modify the functional properties of the NPC or of proteins that are transported through the NPC (e.g., transcription factors) to promote the transformed state. Determining whether the Tpr oncogenic fusions are targeted to the NPC, and, if so, whether NPC localization is required for transformation, should help to resolve this issue.

Localization and Mitotic Dynamics of Tpr

Immunoblot analysis of subcellular fractions from rat liver combined with immunofluorescence staining of cultured cells indicated that Tpr is highly concentrated at the NE. By immunfluorescence microscopy, Tpr was found to have a punctate distribution at the NE that largely colocalized with NPC marker proteins. Immunogold EM on isolated rat liver

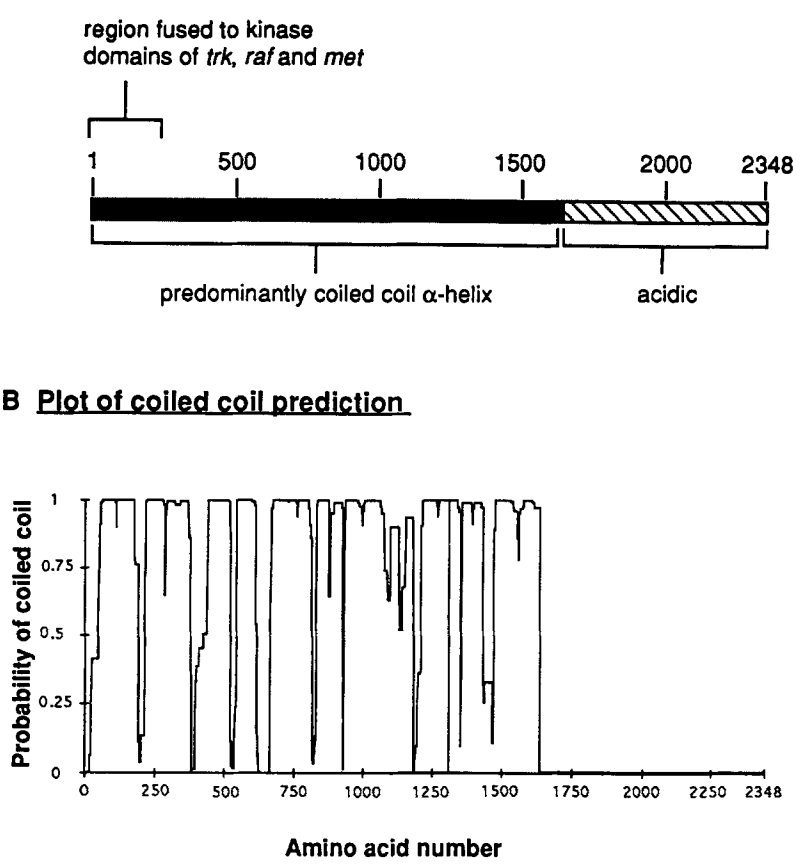

Figure 8. Schematic diagram of human Tpr. The top diagram shows the predicted domain structure of human Tpr (Mitchell and Cooper, 1992*b*) and the bottom plot presents an analysis of the coiled-coil potential of Tpr using the program of Lupas et al. (1991). This method indicates a higher content of coiled-coil in the first 1650 residues of Tpr than suggested by a previous analysis (Mitchell and Cooper, 1992*b*).

NEs confirmed that Tpr is specifically localized to the NPC. Interestingly, Tpr was found to be restricted to the cytoplasmic surface of the NPC, and was most concentrated in regions nearby the cytoplasmic ring. This corresponds to the NPC region occupied by the cytoplasmic fibrils, which by morphological criteria are suggested to be sites where transport ligands initially associate or "dock" with the NPC (Richardson et al., 1988; discussed in Gerace, 1992). In view of the extremely long predicted coiled-coil region of Tpr between residues 50 and 1630, we consider it plausible if not likely that Tpr is part of the backbone of these cytoplasmic fibrils.

If the ~1600-residue long α-helical domain of Tpr forms a continuous two-stranded α-helical coiled coil, its length would amount to ~200 nm (for comparison, see analysis of the lamin rod domain discussed in Gerace and Burke, 1988). However, because of multiple interruptions in the α-helical region of Tpr, it is possible that only a portion of this segment forms a two-stranded α-helical coiled coil, or that the region contains a number of separate domains of this nature joined by flexible linkers. Indeed, four flexible segments within the α-helical domain of Tpr are predicted (Mitchell and Cooper, 1992*b*). If the latter structural model is valid, Tpr-based cytoplasmic fibrils could provide a flexibly jointed "arm" involved in moving transport ligands from their initial docking site at the NPC to the central channel complex, a distance that may exceed 50–100 nm (discussed in Gerace, 1992). Alternatively, it is possible that Tpr is not directly involved in nuclear import and has some other function related to the architecture of the NPC or hypothetical interactions with cytoplasmic structures.

A recent study has identified a 180-kD antigen of the NE that is detected in a variety of vertebrate cells with human autoimmune antibodies (Wilken et al., 1993). In immunoelectron microscopy of isolated NEs of *Xenopus* oocytes, this antigen is localized to the cytoplasmic ring and associated fibrils of the NPC, similar to the localization described here for Tpr. In view of the properties of this 180-kD antigen, including the possible existence of higher molecular mass cross-reacting forms suggested by the published immunoblots (Fig. 1 in Wilken et al., 1993), we consider it likely that this 180-kD antigen corresponds to a proteolytic product of Tpr.

We found that when the NE underwent disassembly during mitosis Tpr was dispersed throughout the cytoplasm, in a similar fashion to NPC proteins studied previously (reviewed by Forbes, 1992; Gerace, 1992). Interestingly, during the period of NE reassembly at the end of mitosis, Tpr associated with the nuclear surface significantly later than the O-linked glycoproteins of the NPC including p62. Almost all of the p62 became concentrated at the reforming NE by early telophase, but most Tpr remained diffusely distributed throughout the cell at this time. Tpr accumulated at the NE only later during mid to late telophase. These results

indicate that assembly of the NPC is a stepwise process, and that formation of peripheral structures containing Tpr follows assembly of other components of the NPC including p62, which is a part of the approximately twofold symmetrical structure of the NPC (see below). However, during the period of early telophase when p62 is concentrated at the NE in the absence of Tpr, it is not clear whether the p62 is assembled into a NPC-like structure or into another assembly intermediate.

Symmetry of the Pore Complex and Nuclear Transport

In addition to Tpr, some O-linked glycoproteins of the NPC have been found to have an asymmetric nuclear/cytoplasmic localization. The CAN protein (von Lindern et al., 1992; Kraemer et al., 1994), as well as an O-linked glycoprotein designated p250 (Panté et al., 1994), have been shown to occur only on the cytoplasmic surface of the NPC (Kraemer et al., 1994; Panté et al., 1994). p250 corresponds to CAN, since it is recognized by polyclonal antibodies raised against the cloned NH_2- and COOH-terminal domains of CAN (Burke, B., and R. Bastos, personal communication). Moreover, the protein Nup153 (Sukegawa and Blobel, 1993), which corresponds to p180 (Snow et al., 1987), is localized exclusively to the nucleoplasmic surface (Snow et al., 1987; Cordes et al., 1993; Sukegawa and Blobel, 1993; Panté et al., 1994). Like Tpr, CAN/p250 (Kraemer et al., 1994; Panté et al., 1994) has been suggested to be associated with the cytoplasmic fibrils, while Nup153/p180 is localized to the nucleoplasmic fibrils (Cordes et al., 1993) in the terminal ring of the nuclear basket (Panté et al., 1994). Thus, the nucleoplasmic and cytoplasmic fibrils, which are structurally distinct peripheral components of the NPC, appear to be at least in part biochemically distinct. By analogy to the putative role of the cytoplasmic fibrils in docking of ligands for nuclear import (Richardson et al., 1988), the nucleoplasmic fibrils may have a docking function in nuclear export.

Apart from the nucleoplasmic and cytoplasmic fibrils, the basic ring-spoke framework of the NPC has twofold symmetry relative to its nucleoplasmic and cytoplasmic "halves" (Hinshaw et al., 1992; Akey and Radermacher, 1993), and these two halves are expected to have similar biochemical compositions. The central channel complex has not yet been analyzed in detail structurally, but it is plausible that it also has twofold symmetry. At least some of the machinery for nuclear import is suggested to have a twofold symmetrical disposition, since the p62 O-linked glycoprotein, which appears to participate directly in nuclear import (Paschal and L. Gerace, manuscript submitted for publication), is localized to both the cytoplasmic and nucleoplasmic surfaces of the NPC (Cordes et al., 1991; Guan, T., et al., manuscript in preparation). Thus, while initial ligand docking at the NPC may involve asymmetric structures that are distinct for import and export pathways (i.e., the cytoplasmic and nucleoplasmic fibrils), many downstream events of transport could involve symmetrically arranged machinery that is used similarly for both import and export pathways. In this context, Tpr might provide a valuable focal point for studying the structural link between initial and more distal steps of nuclear import at the NPC.

We are grateful to George Kleir for assistance with the confocal microscopy, and Christiana Dascher for help with the vaccinia virus expression studies. We also thank Frauke Melchior and Bryce Paschal for helpful comments on the manuscript and Mary Keeter for secretarial assistance.

This work was supported by grants from the National Institutes of Health (L. Gerace), the Swiss National Sciences Foundation and the M. E. Müller Foundation (U. Aebi), and the Human Frontiers Science Program (L. Gerace and U. Aebi). D. Sweet is supported by a Science and Engineering Research Council (United Kingdom) postdoctoral fellowship.

The EMBL/GenBank accession number for the corrected Tpr cDNA sequence is X66397.

Received for publication 15 August 1994, and in revised form 16 September 1994.

References

Adam, S. A., R. E. Sterne-Marr, and L. Gerace. 1990. Nuclear protein import in permeabilized mammalian cells requires soluble cytoplasmic factors. *J. Cell Biol.* 111:807–816.

Akey, C. W., and M. Radermacher. 1993. Architecture of the *Xenopus* nuclear pore complex revealed by three-dimensional cryo-electron microscopy. *J. Cell Biol.* 122:1–19.

Baschong, W., and N. G. Wrigley. 1990. Small colloidal gold conjugated to Fab fragments or to immunoglobulin G as high-resolution labels for electron microscopy: a technical overview. *J. Electron. Microsc. Technol.* 14:313–323.

Cordes, V. C., S. Reidenbach, A. Kohler, N. Stuurman, R. van Driel, and W. W. Franke. 1993. Intranuclear filaments containing a nuclear pore complex protein. *J. Cell Biol.* 123:1333–1344.

Cordes, V., I. Waizenegger, and G. Krohne. 1991. Nuclear pore complex glycoprotein p62 of *Xenopus* laevis and mouse: cDNA cloning and identification of its glycosylated region. *Eur. J. Cell Biol.* 55:31–47.

Davis, L. I., and G. Blobel. 1987. Nuclear pore complex contains a family of glycoproteins that includes p62: glycosylation through a previously unidentified cellular pathway. *Proc. Natl. Acad. Sci. USA.* 84:7552–7556.

Dingwall, C., and R. Laskey. 1991. Nuclear targeting sequences: a consensus? *Trends Biochem. Sci.* 16:478–481.

Fabre, E., and E. C. Hurt. 1994. Nuclear transport. *Curr. Opin. Cell Biol.* 6:335–342.

Feldherr, C., E. Kallenbach, and N. Schultz. 1984. Movement of a karyophilic protein through the nuclear pores of oocytes. *J. Cell Biol.* 99:2216–2222.

Foisner, R., and L. Gerace. 1993. Integral membrane proteins of the nuclear envelope interact with lamins and chromosomes, and binding is modulated by mitotic phosphorylation. *Cell.* 73:1267–1279.

Forbes, D. J. 1992. Structure and function of the nuclear pore complex. *Annu. Rev. Cell Biol.* 8:495–527.

Gerace, L., Y. Ottaviano, and C. Kondor-Koch. 1982. Identification of a major polypeptide of the nuclear pore complex. *J. Cell Biol.* 95:826–837.

Gerace, L., C. Comeau, and M. Benson. 1984. Organization and modulation of nuclear lamina structure. *J. Cell Sci. Suppl.* 1:137–160.

Gerace, L. 1992. Molecular trafficking across the nuclear pore complex. *Curr. Opin. Cell Biol.* 4:637–645.

Gerace, L., and B. Burke. 1988. Functional organization of the nuclear envelope. *Annu. Rev. Cell Biol.* 4:335–374.

Greco, A., M. A. Pierotti, I. Bongarzone, S. Pagliardini, C. Lanzi, and G. Della Porta. 1992. TRK-T1 is a novel oncogene formed by the fusion of TPR and TRK genes in human papillary thyroid carcinomas. *Oncogene.* 7:237–242.

Harlow, E., and D. Lane. 1988. Antibodies: A Laboratory Manual. Cold Spring Harbor Laboratory Press, Cold Spring Harbor, NY.

Hinshaw, J. E., B. O. Carragher, and R. A. Milligan. 1992. Architecture and design of the nuclear pore complex. *Cell.* 69:1133–1141.

Ishikawa, F., F. Takaku, M. Nagao, and T. Sugimura. 1987. Rat c-*raf* oncogene activation by a rearrangement that produces a fused protein. *Mol. Cell. Biol.* 7:1226–1232.

Jarnik, M., and U. Aebi. 1991. Toward a more complete 3-D structure of the nuclear pore complex. *J. Struct. Biol.* 107:291–308.

Konstantinov, K., R. Foisner, D. Byrd, F.-T. Liu, W.-M. Tsai, A. Wiik, and L. Gerace. 1995. Integral membrane proteins associated with the nuclear lamina are novel autoimmune antigens of the nuclear envelope. *Clin. Immunol. Immunopathol.* In press.

Kraemer, D., R. W. Wozniak, G. Blobel, and A. Radu. 1994. The human CAN protein, a putative oncogene product associated with myeloid leukemogenesis, is a nuclear pore complex protein that faces the cytoplasm. *Proc. Natl. Acad. Sci. USA.* 91:1519–1523.

Lupas, A., M. Van Dyke, and J. Stock. 1991. Predicting coiled coils from protein sequences. *Science (Wash. DC).* 252:1162–1164.

Milloning, G. 1961. A modified procedure for lead staining of thin sections. *J. Biophys. Biochem. Cytol.* 11:736–739.

Mitchell, P. J., and C. S. Cooper. 1992*a*. Nucleotide sequence analysis of human *tpc* cDNA clones. *Oncogene.* 7:383–388.

Mitchell, P. J., and C. S. Cooper. 1992*b*. The human *tpr* gene encodes a protein of 2094 amino acids that has extensive coiled-coil regions and an acidic

C-terminal domain. *Oncogene.* 7:2329–2333.
Newmeyer, D., and D. J. Forbes. 1988. Nuclear import can be separated into distinct steps in vitro. Nuclear pore binding and translocation. *Cell.* 51: 641–653.
Newmeyer, D., and D. J. Forbes. 1990. An *N*-ethylmaleimide-sensitive cytosolic factor necessary for nuclear protein import: requirement in signal-mediated binding to the nuclear pore. *J. Cell Biol.* 110:547–557.
Panté, N., and U. Aebi. 1993. The nuclear pore complex. *J. Cell Biol.* 122:977–985.
Panté, N., R. Bastos, I. McMorrow, B. Burke, and U. Aebi. 1994. Interactions and three-dimensional localization of a group of nuclear pore complex proteins. *J. Cell Biol.* 126:603–617.
Park, M., M. Dean, C. S. Cooper, M. Schmidt, S. J. O'Brien, D. G. Blair, and G. F. Vande Woude. 1986. Mechanism of *met* oncogene activation. *Cell.* 45:895–904.
Peters, R. 1986. Fluorescence microphotolysis to measure nucleocytoplasmic transport and intracellular mobility. *Biochem. Biophys. Acta.* 864:305–359.
Reichelt, R., A. Holzenburg, E. L. Buhle, Jr., M. Jarnik, A. Engel, and U. Aebi. 1990. Correlation between structure and mass distribution of nuclear pore complex components. *J. Cell Biol.* 110:883–894.
Richardson, W. D., A. D. Mills, S. M. Dilworth, R. A. Laskey, and C. Dingwall. 1988. Nuclear protein migration involves two steps: rapid binding at the nuclear envelope followed by slower translocation through nuclear pores. *Cell.* 52:655–664.
Rodriguez, G. A., and M. Park. 1993. Dimerization mediated through a leucine zipper activates the oncogenic potential of the *met* receptor tyrosine kinase. *Mol. Cell. Biol.* 13:6711–6722.
Rogers, S., R. Wells, and M. Rechsteiner. 1986. Amino acid sequences common to rapidly degraded proteins: the PEST hypothesis. *Science (Wash. DC).* 234:364–368.
Sawyers, C. L., and C. T. Denny. 1994. Chronic myelomonocytic leukemia: Tel-a-kinase what Ets all about. *Cell.* 77:171–173.
Slot, J. W., and H. J. Geuze. 1985. A new method of preparing gold probes for multiple-labeling cytochemistry. *Eur. J. Cell Biol.* 38:87–93.
Snow, C. M., A. Senior, and L. Gerace. 1987. Monoclonal antibodies identify a group of nuclear pore complex glycoproteins. *J. Cell Biol.* 104:1143–1156.
Soman, N. R., P. Correa, B. A. Ruiz, and G. N. Wogan. 1991. The TPR-MET oncogenic rearrangement is present and expressed in human gastric carcinoma and precursor lesions. *Proc. Natl. Acad. Sci. USA.* 88:4892–4896.
Starr, C. M., M. D'Onofrio, M. K. Park, and J. A. Hanover. 1990. Primary sequence and heterologous expression of nuclear pore glycoprotein p62. *J. Cell Biol.* 110:1861–1871.
Sukegawa, J., and G. Blobel. 1993. A nuclear pore complex protein that contains zinc finger motifs, binds DNA and faces the nucleoplasm. *Cell.* 72:29–38.
von Lindern, M., M. Fornerod, S. van Baal, M. Jaegle, T. de Wit, A. Buijs, and G. Grosveld. 1992. The translocation (6;9), associated with a specific subtype of acute myeloid leukemia, results in the fusion of two genes, dek and can, and the expression of a chimeric, leukemia-specific dek-can mRNA. *Mol. Cell Biol.* 12:1687–1697.
Whiteside, S. T., and S. Goodbourn. 1993. Signal transduction and nuclear targeting: regulation of transcription factor activity by subcellular localization. *J. Cell Sci.* 104:949–955.
Wilken, N., U. Kossner, J.-L. Senecal, U. Scheer, and M.-C. Dabauvalle. 1993. Nup180, a novel nuclear pore complex protein localizing to the cytoplasmic ring and associated fibrils. *J. Cell Biol.* 123:1345–1354.
Wrigley, N. G. 1968. The lattice spacing of crystalline catalase as an internal standard of length in electron microscopy. *J. Ultrastruct. Res.* 24:454–464.